AD-A130 084 A FIELD OF PRESSURES OF SHOCK WAVES DURING A POWERFUL 1/1
UNDERWATER DISCHARGE(U) FOREIGN TECHNOLOGY DIV
WRIGHT-PATTERSON AFB OH G S BONDARENKO 10 JUN 83
UNCLASSIFIED FTD-ID(RS)T-0578-83 F/G 20/4 NL

END
DATE
FILMED
7 83
DTIC

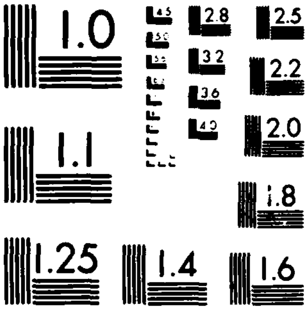

MICROCOPY RESOLUTION TEST CHART
NATIONAL BUREAU OF STANDARDS 1963 A

2

FTD-ID(RS)T-0578-83

# FOREIGN TECHNOLOGY DIVISION

AIR FORCE SYSTEMS COMMAND

## A FIELD OF PRESSURES OF SHOCK WAVES DURING A POWERFUL UNDERWATER DISCHARGE

by

G.S. Bondarenko

FOREIGN TECHNOLOGY DIVISION

Approved for public release;
distribution unlimited.

FTD-ID(RS)T-0578-83

# EDITED TRANSLATION

FTD-ID(RS)T-0578-83 10 June 1983

MICROFICHE NR: FTD-83-C-000740

# A FIELD OF PRESSURES OF SHOCK WAVES DURING A POWERFUL UNDERWATER DISCHARGE

By: G.S. Bondarenko

English pages: 11

Source: Izvestiya Vysshikh Uchebnykh Zavedeniy,
Elektromekhanika, Nr. 5, May 1968,
pp. 503-507

Country of origin: USSR
Translated by: Robert D. Hill
Requester: FTD/TQTD
Approved for public release; distribution unlimited.

PREPARED BY:

TRANSLATION DIVISION
FOREIGN TECHNOLOGY DIVISION
WP-AFB, OHIO.

## U. S. BOARD ON GEOGRAPHIC NAMES TRANSLITERATION SYSTEM

| Block | Italic | Transliteration | Block | Italic | Transliteration |
|---|---|---|---|---|---|
| А а | *А а* | A, a | Р р | *Р р* | R, r |
| Б б | *Б б* | B, b | С с | *С с* | S, s |
| В в | *В в* | V, v | Т т | *Т т* | T, t |
| Г г | *Г г* | G, g | У у | *У у* | U, u |
| Д д | *Д д* | D, d | Ф ф | *Ф ф* | F, f |
| Е е | *Е е* | Ye, ye; E, e* | Х х | *Х х* | Kh, kh |
| Ж ж | *Ж ж* | Zh, zh | Ц ц | *Ц ц* | Ts, ts |
| З з | *З з* | Z, z | Ч ч | *Ч ч* | Ch, ch |
| И и | *И и* | I, i | Ш ш | *Ш ш* | Sh, sh |
| Й й | *Й й* | Y, y | Щ щ | *Щ щ* | Shch, shch |
| К к | *К к* | K, k | Ъ ъ | *Ъ ъ* | " |
| Л л | *Л л* | L, l | Ы ы | *Ы ы* | Y, y |
| М м | *М м* | M, m | Ь ь | *Ь ь* | ' |
| Н н | *Н н* | N, n | Э э | *Э э* | E, e |
| О о | *О о* | O, o | Ю ю | *Ю ю* | Yu, yu |
| П п | *П п* | P, p | Я я | *Я я* | Ya, ya |

*ye initially, after vowels, and after ъ, ь; e elsewhere. When written as ë in Russian, transliterate as yë or ë.

## RUSSIAN AND ENGLISH TRIGONOMETRIC FUNCTIONS

| Russian | English | Russian | English | Russian | English |
|---|---|---|---|---|---|
| sin | sin | sh | sinh | arc sh | sinh$^{-1}$ |
| cos | cos | ch | cosh | arc ch | cosh$^{-1}$ |
| tg | tan | th | tanh | arc th | tanh$^{-1}$ |
| ctg | cot | cth | coth | arc cth | coth$^{-1}$ |
| sec | sec | sch | sech | arc sch | sech$^{-1}$ |
| cosec | csc | csch | csch | arc csch | csch$^{-1}$ |

| Russian | English |
|---|---|
| rot | curl |
| lg | log |

## GRAPHICS DISCLAIMER

# A FIELD OF PRESSURES OF SHOCK WAVES DURING A POWERFUL UNDERWATER DISCHARGE

G.S. Bondarenko

The pressure appearing during an underwater electrical discharge was measured [1, 2, 3, 4, 5, 6], but there is not enough information about it to explain the spatial configuration of the field.

Given at present are results of the study of the dependence of the pressure at the front of the shock wave on the radial and angular coordinates with the simultaneous recording of the current and voltage and also the electroacoustic efficiency of the discharge.

The pulse voltage generator and the equipment used for measuring the pressure of the electrical characteristics are described in [4]. The measuring equipment was supplemented by a compensator of inductive shift of the current and voltage phases. Resistors of the VS type were used in the high-voltage arm of the divider.

The discharge device with the electrodes knife (plus) and plate (minus), attached on a movable frame, can be turned around an axis perpendicular to the direction of the discharge and passing through the middle of the discharge interval. This made it possible to change the angle between the axis of the discharge and direction to the measuring hydrophone from 0° to 180°. The discharge axis was conditionally directed from the positive electrode to the negative. The cable core RK 103 was used as the positive electrode.

The triggering and measuring hydrophones were assembled on a movable plexiglass plate, which could be moved over a guide along a bath. This provided a change in the distance to the discharge channel of 30 cm to 80 cm.

In the measuring microphone the sensing element was made in the form of a cylinder of ceramics of barium titanite with an outer diameter of 2.2 mm, wall thickness of 0.3 mm and height of 4 mm. A piezoelectric element was attached to a syringe needle by means of an epoxy resin. The housing of the needle was soldered to a wire connected with the internal wall of the element. The insulated wire, connected with the inner facing, was passed through the channel of the needle and soldered with the cable core. The rim of the needle was soldered to the shield of the cable. For the start of the sweep, a microhydrophone with a spherical piezoelement with a diameter of 4 mm was used.

For the measuring microhydrophones used, the upper limit of the passband was 700 Hz, which corresponded to a time constant with respect to high frequencies of 1.5 $\mu$s.

The calibration of the microhydrophones was conducted by the quasi-static method.

Used in the investigation were storage capacitances of 0.2, 0.5, 1, 3, and 4 $\mu$F and discharge voltages of 30, 40, 50, and 70 kV. The liquid gap varied from 30 mm to 50 mm. This allowed obtaining periodic, aperiodic and transient dischargers.

As an example Fig. 1 gives voltage and current oscillograms for the discharge of $V=50$ kV, $C=1$ $\mu$F, and $l=50$ mm.

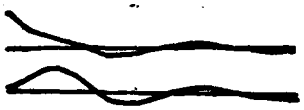

Fig. 1. Voltage and current oscillograms: $C=1$ $\mu$F, $V=50$ kV and $l=50$ mm.

At an initial voltage of 50 kV, the discharge current reaches a maximum value of $3.6\cdot10^{4}$ A with a slope rise of $10^{10}$ A/s. The discharge is periodic with a logarithmic decrement of attenuation of

$\vartheta=0.933$.

The effective resistance of the channel, calculated according to the decrement, consists of $R_{\text{эф}}=0.42$ ohms. Curves of the electrical power released into the channel are plotted according to the obtained voltage and current oscillograms. The maximum power for the discharge of $V=50$ kV, $C=1$ $\mu$F, and $l=50$ mm, reachable in the first half-period, is $23.8\cdot10^{7}$ W with the slope rise of $\gamma=2.48\cdot10^{13}$ W/s.

The slope of the power referred to the length of the channel is

$$\frac{\gamma}{l}=4{,}96\cdot10^{14}\ \text{W/ms}.$$

The calculation shows that with the used discharge parameters, in the first half-period 70% of all the energy stored in the circuit is released into the channel.

Figure 2 gives pressure oscillograms of shock waves for distances of 30, 40, 50, 60, 70, and 80 cm when $\Theta=90°$ ($V=50$ kV, $C=1$ $\mu$F, and $l=30$ mm). For each position of the microhydrophone, 5-7 photographs were taken. The good repetition of the oscillograms should be noted.

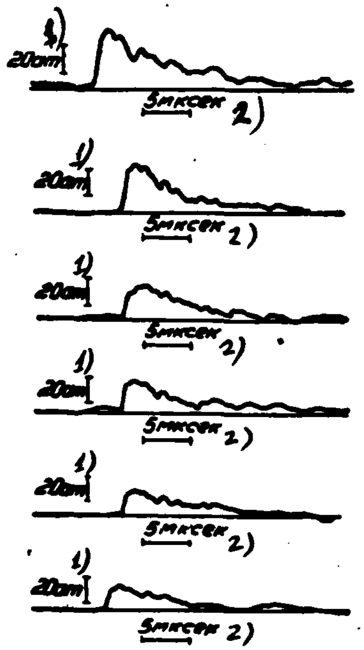

Fig. 2. Pressure oscillograms of shock waves for distances of 30, 40, 50, 60, 70, and 80 cm, $\Theta=90°$. Key: 1) at; 2) $\mu$s.

It is easy to see that with a change in the distance from the discharge axis, the shape of the pulse is substantially not changed.

Figure 3 gives a graph of the dependence of pressure at the front of the shock wave on distance. For the conditions being investigated, this dependence corresponds to the acoustic law and can be expressed by the empirical formula

$$P=\frac{a}{r},$$

where a is the coefficient dependent on the discharge parameters. For the conditions of V=50 kV, C=1 μF, *l*=50 mm, a=13.16 at.m. [Sic. Translator's note: this is the abbreviation for "atomic mass;" it could be an error in the original; could also stand for at/m.]

Figure 4 gives pressure oscillograms for angles of 90°, 45° and 15° (V=50 kV, C=1 μF, and *l*=30 mm). With an increase or decrease in angle θ relative to angle θ=90°, the slope of the pulse front is decreased, the pulse acquires a trapesoidal shape, the pulse duration grows, and the front of the wave often becomes nonshock.

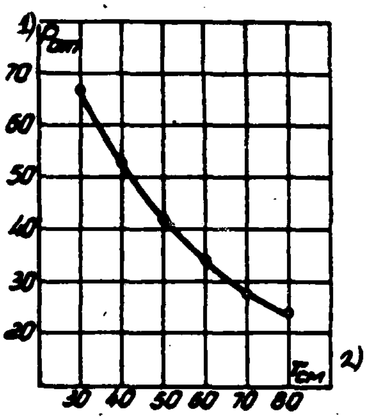

Fig. 3.

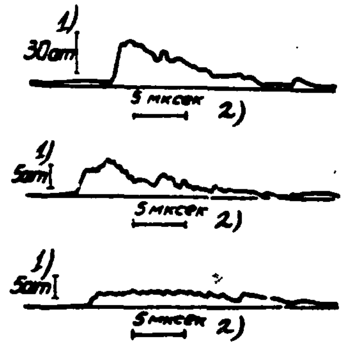

Fig. 4.

Fig. 3. Dependence of pressure at front of shock wave on distance. Key: 1) P(at); 2) T(cm).

Fig. 4. Pressure oscillograms at θ=90°, 45°, 15°, and r=80 cm. Key: 1) at; 2) μs.

Curves of the dependence of pressure on the angular coordinate θ when r=40 cm and 80 cm are given on Fig. 5. From the curves it follows that the pressure receives the maximum value when θ=90°, reaching minimal values when θ=180° and 0°. It follows to note a certain assymetry of pressures relative to the direction θ=90°, which, apparently, is connected with design characteristics of the discharge device. A comparison of the curves for different distances shows that at distances closer to the channel, the maximum of pressure when θ=90° is more greatly expressed. This means that with departure of the shock wave from the channel, the angular dependence of pressure is weakened, and the pressure field approaches spherically symmetric.

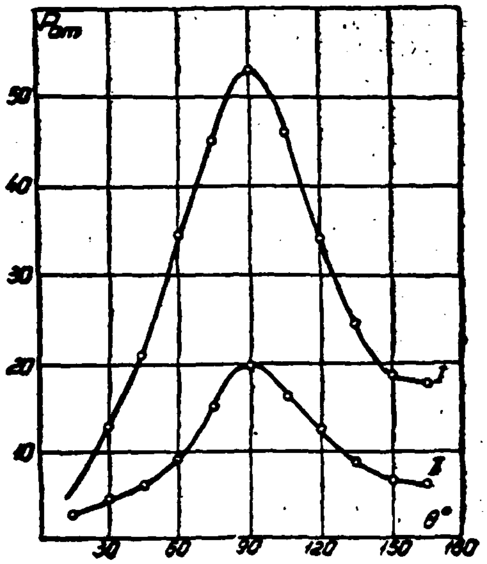

Fig. 5.

Fig. 5. Dependence of pressure on the angular coordinate Θ.

The electroacoustic efficiency $\eta_a$ is determined as the ratio of energy of the shock wave moved through a sphere with a radius of 0.8 m to the energy stored in the storage capacitance of the circuit.

To explain the energy of the shock wave, the area of the sphere is divided into 11 zones. The pressure pulse was considered symmetrical with respect to the axis of the discharge. The pressure was determined as an average in the center of each zone.

For each zone the energy was calculated according to the formula

$$W_{з} = S_{з}\frac{1}{\rho_0 c_0}\sum_{i=1}^{n} P_i{}^2 \Delta t_i,$$

where $S_з$ is the area of the zone, $P_i$ - the pressure, $\rho_0 c_0$ - the wave impedance of the water, and Δt - the time interval during which the pressure did not undergo significant changes and, therefore, could be taken as constant. The pressure pulse was divided into 20-30 such intervals.

The total energy was found as the sum of the energies moved through all the zones.

Besides the electroacoustic efficiency, we calculated the so-called electrohydrodynamic efficiency for the stage of the steady-state expansion of the channel ($\eta_{\text{э}}$), equal to the ratio of the energy of the shock wave to the energy introduced into the channel in this stage. Obtained in reference [5] is the theoretical formula for the calculation of the electrohydrodynamic efficiency.

In this investigation the electrohydrodynamic efficiency was determined as the ratio of the energy of the shock wave to the energy released into this channel during the build-up of electrical power. Power curves plotted on current and voltage oscillograms were used for the calculation.

Results of the measurements are given in the table.

| №№ режима 1) | 2) Параметры | | | Запас энергии, дж 6) | Число полупериодов тока 7) | Энергия, выделенная в канал, дж 8) | Энергия ударной волны, дж 9) | $\eta_a$, % | $\eta_{\text{э}}$, % |
|---|---|---|---|---|---|---|---|---|---|
| | V, кв 3) | C, мкф 4) | l, мм 5) | | | | | | |
| 1 | 50 | 4 | 50 | 5000 | 5 | 1419 | 231 | 4,8 | 16 |
| 2 | 50 | 1 | 50 | 1250 | 3 | 510 | 112 | 9 | 10 |
| 3 | 50 | 1 | 30 | 1250 | 6 | 336 | 90 | 7,2 | 27 |
| 4 | 50 | 0,2 | 50 | 250 | 2 | 103 | 23,5 | 9,5 | 23 |
| 5 | 40 | 1 | 50 | 800 | 3 | 360 | 95,6 | 12 | 26 |
| 6 | 30 | 1 | 40 | 450 | 1 | 167 | 44 | 6,7 | 18 |
| 7 | 70 | 0,2 | 50 | 490 | 3 | 163 | 45 | 9 | 27 |
| 8 | 70 | 1 | 50 | 2450 | 7 | 590 | 168 | 7 | 30 |

Table Key: 1) No. of mode; 2) Parameters; 3) kV; 4) μF; 5) mm; 6) Energy reserve, J; 7) Number of current half-periods; 8) Energy released into the channel, J; 9) Energy of shock wave, J.

From the obtained data it follows that the electroacoustic efficiency for the investigated modes varies from 5% to 12%.

By analyzing the results, it is possible to draw the conclusion that $\eta_a$ depends, first of all, on the nature of the discharge; the highly periodic discharges possess low efficiency. The same pertains to the purely aperiodic discharge (mode No. 6).

The maximal efficiencies take place for the transient discharges with 2-3 periods of current. Quantity $\eta_a$ is increased with a decrease in capacitance at constant voltage and length of the discharge gap $l$.

A comparison of the power curves obtained for the different modes with values of $\eta_a$ and also $\eta_w$ shows that the modes possessing high efficiencies have a well-marked linearity of the increasing part of the power curve. Modes Nos. 1-6 possess the least efficiencies. Curves of electrical power corresponding to these modes are distinguished by a considerable nonlinearity of the ascending part, which hinders the theoretical calculation of the electrohydrodynamic efficiency.

From the obtained results on the investigation of efficiency, the following conclusions can be drawn:

1. Electroacoustic efficiency of an underwater discharge for the investigated modes does not exceed 12%.

2. Transient discharges with two to three half-periods of current possess the greatest efficiency.

3. The efficiency is decreased with an increase in the storage capacitance.

Manuscript received: initially on 16 November 1967 and after revision - 20 February 1968.

## References

1. Рой Н. А. и Фролов Д. П., „Об электроакустическом к.п.д. искрового разряда". Докл. АН СССР, 1958, т. 118, № 4, стр. 683.
2. Воротникова М. И., „Влияние скорости тепловыделения при электровзрыве в воде на распределение энергии взрыва". ПМТФ, 1962, № 2, стр. 110.
3. Баженова Т. В. и Солоухин Р. И., „Поле давлений, возникающее в воде при электрическом разряде. „Физическая газодинамика" (Энергетический институт им. Г. М. Кржижановского), М., Изд-во АН СССР, 1959.
4. Арсентьев В. В., Богданов Н. И., Установка для исследования импульсных разрядов в жидкой среде. „Акустическая и магнитная обработка веществ". Сб. статей, Новочеркасск, 1966.
5. Арсентьев В. В., „К теории импульсных разрядов в жидкой среде". ПМТФ, 1965, № 5, стр. 51.
6. Страхов Ю. М., Либенсон В. А., Файнберг Г. С., „Исследования характеристик ударной волны, возникающей при электрическом разряде в воде". Труды ВНИИОМШСа, выпуск 16, изд-во „Недра", М., 1965, стр. 105.